Parameters optimization for the generation of a keyhole weld pool during the start-up segment in variable-polarity plasma arc welding of aluminium alloys

B Zheng[1], **Q l Wang**[2] and **R Kovacevic**[1]*
[1]Department of Mechanical Engineering, Southern Methodist University, Dallas, Texas, USA
[2]Harbin Institute of Technology, Harbin, People's Republic of China

Abstract: Stable weld formation is still one of the goals pursued in variable-polarity plasma arc welding (VPPAW) of aluminium alloys. Basically, VPPAW is divided into three segments: the start-up segment, during which the keyhole is generated, the main body segment, during which the keyhole is dynamically maintained, and the terminal segment, during which the keyhole collapses and the crater is filled. Very often, a smooth transition cannot be made from the start-up segment to the main body segment, and the weld easily fails because the keyhole weld pool is not properly generated. This paper explores four different combinations of plasma gas and welding current for generating a smooth transition from the start-up segment to the main body segment in VPPAW. The keyhole weld pool is categorized as one of three types: heat conduction mode, strong force mode or heat and force mode. The heat and force mode of the keyhole weld pool can be generated by raising the gas flowrate, raising the current or by raising both the gas and current. An increase in the plasma gas flowrate accompanied with an increase in the welding current is the best combination for generating a smooth transition during the start-up segment, which results in only a few double arcs and no short circuiting between the nozzle and the workpiece. The quality of the initial weld bead can be guaranteed using this approach.

Keywords: VPPAW, aluminium, keyhole weld pool, start-up weld bead, parameters optimization

1 INTRODUCTION

Aluminium is one of the widely used important structural materials in industry. Because of its highly reactive nature, aluminium is almost never found in nature in its free state. Of particular note is its affinity for oxygen: aluminium typically has a surface layer of aluminium oxide that is 100–200 billionths of an inch (25–50 Å) thick. This tenacious oxide film on aluminium strongly impedes the flow of molten metal in the weld pool during welding and leads to the formation of very poor welds containing oxide inclusions. Another difficulty associated with aluminium welding is that the aluminium will absorb a high quantity of hydrogen when it melts (almost a twentyfold increase in solubility). As the weld pool solidifies, the absorbed hydrogen is forced out of solution and becomes trapped in the weld bead, generating hydrogen porosity inside the weld [**1**, **2**].

Variable polarity plasma arc welding (VPPAW) features a combination of a direct current (d.c.) electrode negative (DCEN) period and a d.c. electrode positive (DCEP) period in a single cycle. Thus, it is an alternating current (a.c.) welding process. In the DCEN period, the concentrated arc can deeply penetrate the workpiece, while the DCEP arc can remove the oxide film on the workpiece surface by the bombardment from the heavy ions travelling to the workpiece. Using this so-called cathodic cleaning action from a DCEP arc, which is associated with the keyhole mode of penetration, a nearly porosity-free weld bead can be achieved. Owing to its high quality and low cost [**3**–**6**], this welding process is particularly suitable for the fabrication of critical products, such as the external fuel tank for the space shuttle, missile shells and nuclear magnetic resonance devices.

The MS was received on 25 February 1999 and was accepted after revision for publication on 4 August 1999.
**Corresponding author: Department of Mechanical Engineering, Southern Methodist University, PO Box 750337, Dallas, TX 75275, USA.*

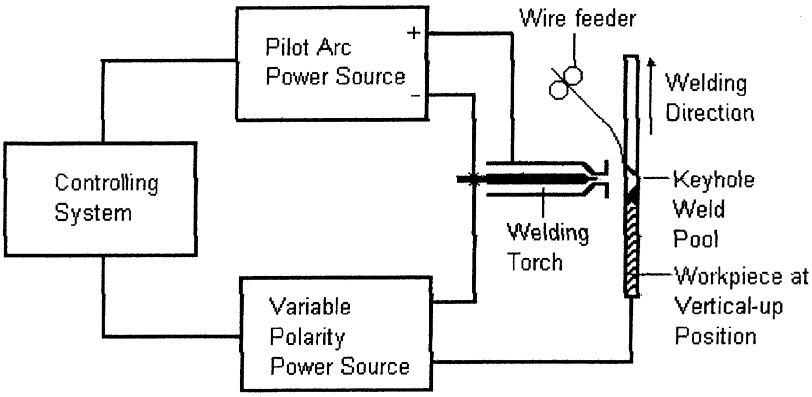

Fig. 1 Block diagram of variable-polarity plasma arc welding system

At present, stable weld formation is still one of the goals pursued in VPPAW of aluminium alloys. Basically, the welding process is divided into three segments: the start-up segment, during which the keyhole is generated, the main body segment, during which the keyhole is dynamically maintained, and the terminal segment, during which the keyhole collapses and the crater is filled. Very often, a smooth transition cannot be made from the start-up segment to the main body segment, and the weld easily fails because the keyhole weld pool is not properly generated.

In previous research, most investigators have focused their attention on the cleaning action of the DCEP arc [**7**–**9**], arc stability [**10**, **11**], the melting behaviour of the weld pool [**12**, **13**], monitoring keyhole stability and penetration control during the main body segment [**14**–**19**], etc. However, smooth transition from the start-up segment to the main body segment has not been fully investigated. Occasionally, the approach of drilling a hole at a weld start location for easy generation of a keyhole has been adopted, which in some cases is unacceptable and may result in inefficient melting at this point. In the present paper, different combinations of parameters for generating different modes of the keyhole weld pool during the start-up segment are investigated.

2 EXPERIMENTAL PROCEDURE

2.1 Experimental set-up

The welding system shown in Fig. 1 consists of a variable-polarity welding power source of 300 A, a programmable sequence controller, a plasma gas controller, a computer numerical control (CNC) positioning system, a wire feeder and a plasma torch.

2.2 Experimental conditions

In order to achieve plasma arc welding with the keyhole mode, the combination of three crucial parameters should be optimized: welding current, plasma gas flowrate and welding speed. Because the welding speed is usually maintained constant during the welding process, the welding current and plasma gas flowrate are selected to be the variable parameters. Effects of the following combinations are explored (shown in Fig. 2): a constant plasma gas flowrate with a constant welding current, an increase in the plasma gas flowrate with a constant welding current, a constant plasma gas flowrate with increase in the welding current, and increases in both the plasma gas flowrate and the welding current. Bead-on-plate

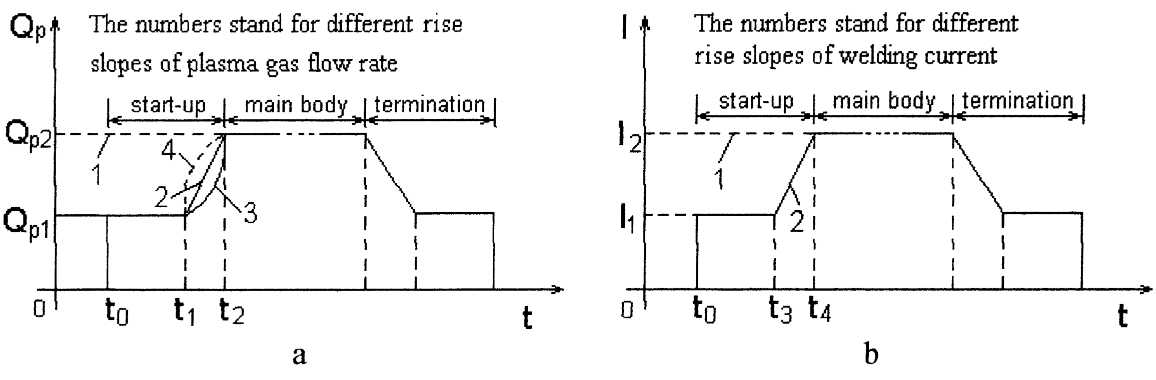

Fig. 2 (a) Plasma gas flowrate Q_p and (b) welding current I versus time: t_0 instant of plasma arc initiation; t_1 instant of plasma gas increase; t_2 instant of plasma gas increase stop; t_3 instant of welding current increase; t_4 instant of welding current increase stop

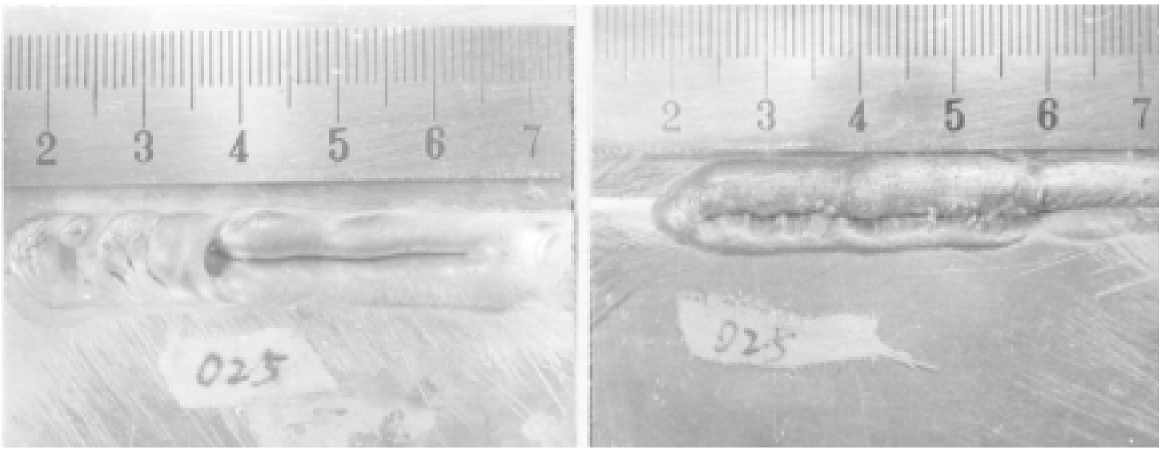

a b

Fig. 3 Photographs of the weld bead when a cutting process occurs with the constant mode: (a) front side; (b) back side

welds without filler metal are made on 6.0 mm thick 2024 aluminium alloy plates in a vertical-up position. The welding parameters are as follows: initial welding current 115–130 A, maximum welding current (at the end of the start-up segment) 145–150 A, plasma gas flowrate rise time 0–21 s, welding current rise time 0–10 s, torch stand-off distance 5.0–6.0 mm, nozzle diameter 4.0 mm, shielding gas flowrate 4.5×10^{-3} m^3/min, and welding speed 6.3 cm/min.

3 EXPERIMENTAL RESULTS

Based on the experiment, a smooth transition of the welding process from the start-up segment to the main body segment features the following:

(a) absence of double arcs and low arc noise;
(b) no oxidation in the melting zone and its surrounding area;
(c) moderate keyhole size, i.e. small enough to prevent cutting of the workpiece and large enough to avoid collapsing when torch movement begins;
(d) the solidified metal at the starting point and at the rear of the keyhole is not so high that short circuiting between the nozzle and workpiece occurs;
(e) guaranteed weld quality at the start location.

3.1 Constant plasma gas flowrate with a constant welding current

When both the plasma gas flowrate and the welding current during the start-up segment are respectively set at a value of less than or equal to Q_{p2} (the value for the main body segment, curve 1 in Fig. 2a) and at I_2 (the value for the main body segment, curve 1 in Fig. 2b), the welding process is unstable. This combination of parameters is defined in this paper as the constant mode. The metal in the weld pool is forced to go up towards the nozzle because of the digging effect of the high arc force, which often results in double arcs or short circuiting between the nozzle and workpiece. Often, the weld bead behind the keyhole cannot be formed when the workpiece begins to move, which results in a cutting process, as shown in Fig. 3.

3.2 Increase in the plasma gas flowrate with a constant welding current

When the plasma gas flowrate increases from an initial value of Q_{p1} to a value of Q_{p2} for the main body segment (curve 2 or 3 in Fig. 2a) and the welding current is set at I_2 (curve 1 in Fig. 2b), the parameters influencing the formation of a keyhole weld pool are: Q_{p1}, Q_{p2}, the duration of the initial plasma gas flowrate period, t_1, and the

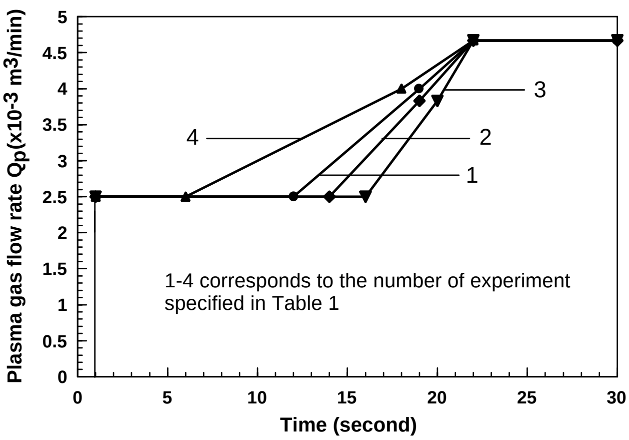

Fig. 4 Relationship between plasma gas flowrate and time during the start-up segment using the gas rise mode

Table 1 Plasma gas flowrate and its rise time during start-up segment

Number of experiment	Preheat time t_1 (s)	Instant of keyhole formation (s)	Instant of stopping plasma gas flowrate increase t_2 (s)	Plasma gas flowrate increase time $t_2 - t_1$ (s)	Plasma gas flowrate at keyhole formation (10^{-3} m^3/min)
1	11	18	21	11	4.00
2	13	18	21	8	3.83
3	15	19	21	8	3.83
4	5	17	21	18	4.00

*$Q_{p1} = 2.50 \times 10^{-3}$ m^3/min, $Q_{p2} = 4.67 \times 10^{-3}$ m^3/min, $I_1 = I_2 = 145$ A, welding speed $V_s = 8.30$ cm/min.

duration of the plasma gas flowrate period $(t_2 - t_1)$. This combination is defined in this paper as the gas rise mode. The results showed that the initial plasma gas flowrate Q_{p1} and the main body plasma gas flowrate Q_{p2} should be experimentally selected on the basis of the thickness of the workpiece and the welding speed. Using the appropriate plasma gas flowrate, a stable welding process and high weld quality can be guaranteed during the transition from the start-up segment to the main body segment. Figure 4 shows the increasing curves of plasma gas flowrate, which were drawn on the basis of the data in Table 1. A photograph of the weld bead corresponding to curve 1 in Fig. 4 is shown in Fig. 5, which illustrates the unfavourable tower-shaped metallic solidification at the starting location on the back side of the workpiece.

3.3 Constant plasma gas flowrate with an increase in the welding current

In most cases, a stable keyhole weld pool can be achieved during the start-up segment, when the initial plasma gas flowrate is kept constant at Q_{p2} (curve 1 in Fig. 2a) and the welding current increases from an initial value of I_1 to I_2 (curves 1 and 2 in Fig. 2b, respectively). This combination of parameters is defined in this paper as the current rise mode. The time for initial welding current is 5–10 s and the time for welding current increase is in the range 0–10 s. However, sometimes the welding process is unstable if the time for welding current increase is set at zero (i.e. welding current steps from I_1 to I_2). Using this combination of parameters, a smooth transition from the start-up segment to the main body segment can be generated and the unfavourable tower-shaped metallic solidification at the start location of the weld bead can be left on the front side of the workpiece.

3.4 Increases in both the plasma gas flowrate and the welding current

The generation of a smooth transition from the start-up segment to the main body segment can be optimized by increasing both the plasma gas flowrate and the welding current, which is defined in this paper as the gas–current rise mode (curve 2 in Fig. 2a and Fig. 2b respectively). The parameters influencing the keyhole weld pool at the start-up segment are: the initial plasma gas flowrate and the initial welding current (associated with their acting time), the intervals between the start of increase in the plasma gas flowrate and the welding current, and the terminating values for the plasma gas flowrate and the welding current. Typical experimental data are shown in Table 2, on the basis of which the relationship between the welding current and the plasma gas flowrate versus time is derived (Fig. 6).

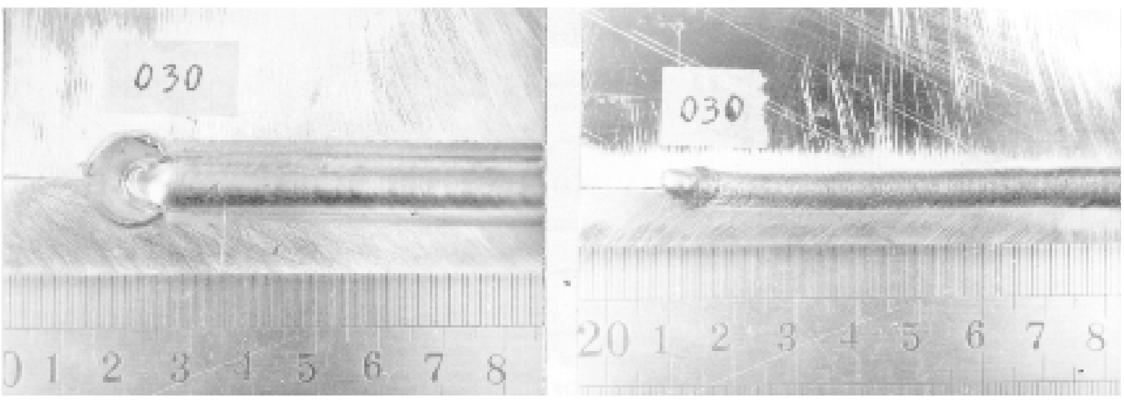

a b

Fig. 5 Photographs of the weld bead with the gas rise mode during the start-up segment (corresponding to experiment 1 in Table 1): (a) front side; (b) back side

Table 2 Plasma gas flowrate, welding current and their rise times

Number of experiment	t_1 (s)	$t_2 - t_1$ (s)	t_3 (s)	$t_4 - t_3$ (s)	Q_{p1} (m^3/min)	Q_{p1} (m^3/min)	I_1 (A)	I_2 (A)	Remarks
1	5	10	10	5	2.5×10^{-3}	3.7×10^{-3}	130	140	Double arc, without short circuiting; flat front side, but tower-shaped back side
2	10	5	10	10	2.5×10^{-3}	3.5×10^{-3}	115	140	Double arc, without short circuiting; both front side and back side are flat
3	5	10	10	0	2.5×10^{-3}	3.5×10^{-3}	130	140	Double arc; sharply tower-shaped front side, but flat back side
4	5	10	5	10	2.5×10^{-3}	3.5×10^{-3}	130	140	Double arc; flat front side, but sharp tower-shaped back side

*Welding speed $V_s = 10.0$ cm/min.

The experiment also showed that the following guidelines should be used for matching the above parameters, although a stable welding process and quality weld bead may be achieved using the data in Table 2:

1. The instant for increasing the plasma gas flowrate, t_1, should come before the welding current increase, t_3, and the workpiece preheat, depending on t_3, should be reasonable (this means that t_3 cannot be significantly changed). If t_1 is less than t_3, the balance between the arc and the weld pool cannot be easily maintained; double arcs and short circuiting between the nozzle and workpiece can occur.
2. The rise time for the plasma gas flowrate, $t_2 - t_1$, may be shorter or longer than the rise time for the welding current, $t_4 - t_3$.
3. The initial and terminated values for the plasma gas flowrate and the terminated welding current may not be randomly selected, but the initial welding current can be selected in the range 115–130 A.

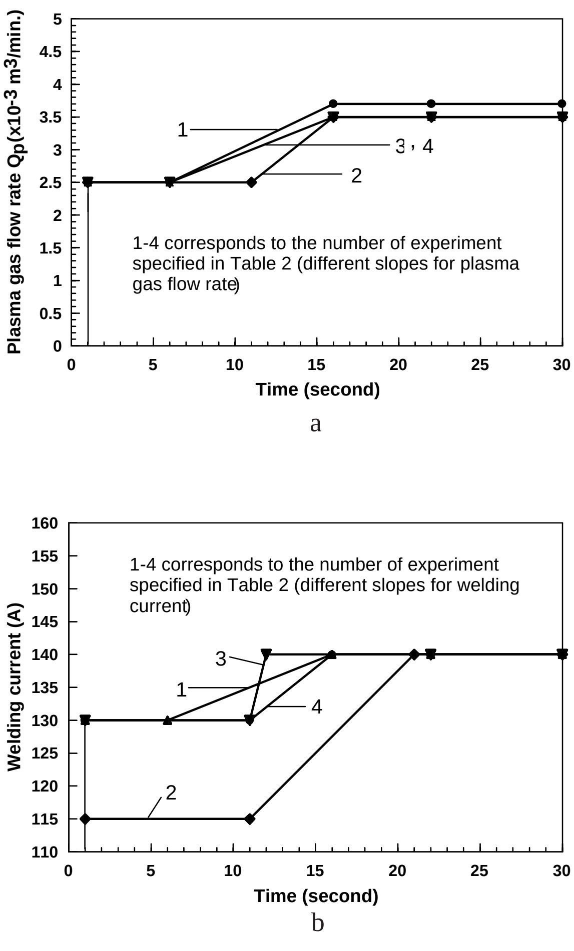

Fig. 6 (a) Plasma gas flowrate and (b) welding current versus time during the start-up segment using the gas–current rise mode

By allowing a longer period for the initial plasma gas flowrate, t_1, and a shorter period, $t_2 - t_1$, for increasing the plasma gas flowrate, the ideal welding process and optimum weld bead without double arcs and unfavourable tower-shaped metallic solidification can be achieved. This is true only if the increase in the initial welding current is postponed (i.e. t_3 is increased) and if the rise time for the welding current is increased (i.e. $t_4 - t_3$ is increased). Weld bead photos corresponding to this type of parameter combination for experiment 2 in Table 2 are shown in Fig. 7.

4 DISCUSSION

The keyhole formation is a dynamic process in which the arc heat melts the base metal and the arc force applied to the melted zone digs the liquid metal and pierces a hole through the weld pool. This process depends not only on the heat and force from the arc but also on their changing speed, so the factor of time should be considered. The initial welding current and its duration determine the effectiveness of preheat at the start location on the workpiece. Preheat of the start location can result in an initial small-sized weld pool, and can also form an appropriate temperature gradient between it and the heat-affected zone. Since an aluminium alloy is a heat-sensitive material, the weld pool is easily burnt through during the keyhole formation if too much heat is input to it, and the temperature gradient between the weld pool and heat-affected zone is too small because of the preheat. However, double arcs and/or short circuiting easily occur during keyhole formation if too

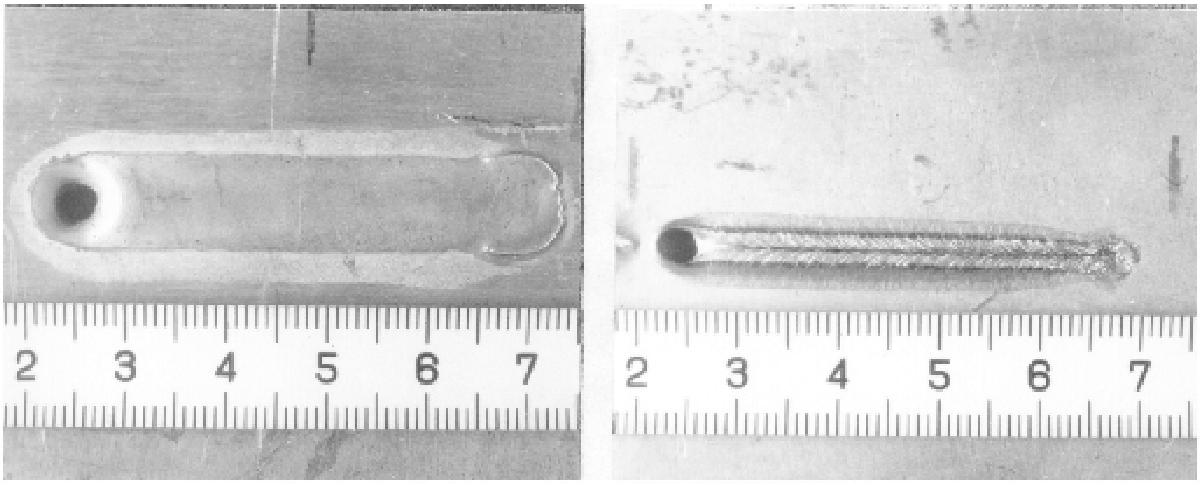

Fig. 7 Photographs of the weld bead with matched gas and welding current rise slopes during the start-up segment (corresponding to experiment 2 in Table 2): (a) front side; (b) back side

little heat is input to it, and the above-mentioned temperature gradient is too large because of the preheat (for instance, in the case of the constant mode if Q_p and I are both set at the values for the main body segment). When the appropriate preheat and a moderate increase in the plasma gas flowrate are applied, the arc force increases and becomes concentrated (this is helpful for forming the keyhole). However, the arc force can depress the liquid metal moving towards the nozzle. In the case of the current rise mode, the quantity of melted metal is increased. As the welding current increases, the molten metal first moves towards the nozzle and then down to the rear of the keyhole on the workpiece surface, owing to gravity and the vertical-up welding position. Because double arcs and short circuiting can easily occur if the liquid metal is not depressed by an appropriate arc force, the slope of the welding current increase needs to be properly selected. In the gas–current rise mode, the weld pool metal moving towards the nozzle can be depressed and transformed into a dish-like shape if the plasma gas flowrate is increased before the welding current and their rates of increase are matched. The schematic is shown in Fig. 8. The keyhole formation is stable, and the transition from the start-up segment to the main body segment is smooth. Double arcs and short circuiting between the nozzle and workpiece seldom occur. In this case, a flat weld bead on both the front and back side at the start location may be achieved.

It was found that the plasma gas flowrate can be increased according to curve 4 in Fig. 4, which is more reasonable for the stable establishment of a keyhole weld pool and a smooth transition. Also, if the plasma gas flowrate increases according to dashed curve 4 in Fig. 2, the keyhole easily collapses at the start-up segment as the workpiece begins to move.

As shown in Fig. 9, the keyhole weld pool at the start-up segment can be categorized as one of three types: heat conduction mode, strong force mode or heat and force mode. The reason for generating a heat conduction mode is that the weld pool melts through mainly by heat accumulation in the workpiece (because of the low initial welding current and long acting time). The stable formation of a keyhole, associated with few double arcs and a stable weld pool, takes a long time. The tower-shaped metallic solidification at the back side of the workpiece is large when the keyhole forms. Also, the cutting process easily occurs when the workpiece starts to move. A higher plasma gas flowrate accompanied with a lower initial welding current and a shorter rise time of the welding current will result in a higher and more concentrated arc force, which will generate a

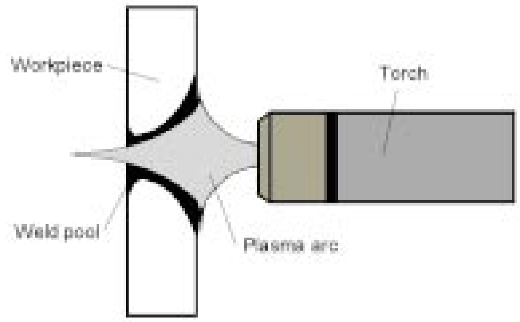

Fig. 8 Schematic of plasma arc and weld pool when the keyhole is generated during the start-up segment in PAW

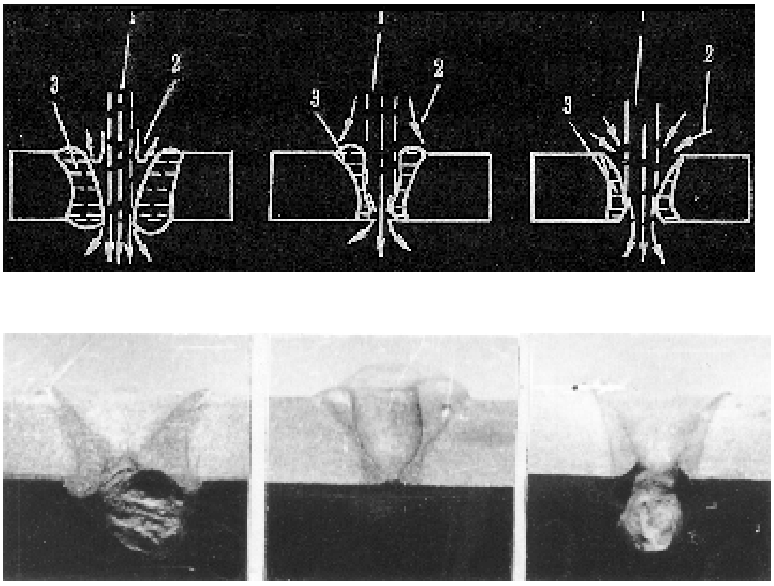

a b c

Fig. 9 Sketches and photographs of different keyhole modes during the start-up segment in PAW: (a) heat conduction mode; (b) strong force mode; (c) heat and force mode; 1, plasma arc; 2, supplementary gas; 3, weld pool

strong force mode weld pool. Unstable keyhole generation is often associated with a double arc and short circuiting. After the small, trumpet-shaped keyhole forms, less molten metal can go to the back side of the workpiece through the keyhole to form the tower-shaped metallic solidification. Also, the keyhole easily collapses when the workpiece begins to move. The heat and force mode can be achieved by the appropriate heat accumulation and the proper temperature gradient between the weld pool and the heat-affected zone. The efflux through the keyhole cannot expand freely because of the limited sizes of the weld pool and the keyhole. Using this mode, the transition from the start-up segment to the main body segment is smooth and the as-welded result is good.

5 CONCLUSION

The smooth transition from the start-up segment to the main body segment is one of the crucial factors influencing stable weld formation in variable-polarity plasma arc welding of aluminium alloys with the keyhole mode. An increase in the plasma gas flowrate accompanied with an increase in the welding current will generate a smooth transition during the start-up segment, with few double arcs and no short circuiting between the nozzle and the workpiece. The quality of the weld bead can be guaranteed at the start-up location using this ideal approach.

ACKNOWLEDGEMENTS

The authors wish to thank the National Key Laboratory of Advanced Welding Production Technology, Harbin Institute of Technology, People's Republic of China, the Department of Mechanical Engineering of Southern Methodist University, Dallas, Texas, and NSF (Grant DMI-9900011) for their funding and support.

REFERENCES

1 **Craig, E.** The plasma arc process—a review. *Weld. J.*, 1988, **2**, 19–25.
2 **Tuttle, W.** Understanding aluminum welding. *Weld. J.*, 1991, **70**, 43–46.
3 **Tomsic, M.** and **Barhost, S.** Keyhole plasma arc welding of aluminum with variable polarity power. *Weld. J.*, 1984, **63**(2), 25–27.
4 **Nunes, C.** and **Bayless, E. O.** Variable polarity plasma arc welding on space shuttle external tank. *Weld. J.*, 1984, **63**(4), 27–35.
5 **Woodward, H.** A U.S. contractor for the International Space Station. *Weld. J.*, 1996, **3**, 35–40.
6 **Irving, B.** Joining experts meet to exchange ideas about welding in space. *Weld. J.*, 1992, **1**, 67–69.
7 **Barhorst, S.** The cathodic etching technique for automated aluminum tube welding. *Weld. J.*, 1985, **5**, 28–31.
8 **Kyselica, S.** High-frequency reverse arc switch for plasma arc welding of aluminum. *Weld. J.*, 1987, **1**, 31–35.

9 **Pang, Q.,** *et al*. Workpiece cleaning during variable polarity plasma arc welding of aluminum. *Trans. ASME, J. Engng for Industry*, 1994, **116**(11), 463–466.

10 **Zheng, B.** The discontinuous pilot power source for AC PAW. *China Weld*., 1995, **6**, 1–6.

11 **Zheng, B., Wang, Q. L.** and **Kovacevic, R.** Arc interference and a unique push-pull-arc solution in AC PAW of aluminum alloys. *J. Engng Mf*., 1999 (accepted).

12 **Torres, M. R.** Gas contamination effects in variable polarity plasma arc welded aluminum. *Weld. J*., 1992, **4**, 123–130.

13 **Martinez, L. F.** Effect of weld gases on melt zone size in VPPA welding of Al 2219. *Weld. J*., 1994, **10**, 50–55.

14 **Steffens, H. D.** Automatic control for plasma arc welding with constant keyhole. *Weld. J*., 1972, **6**, 40–45.

15 **Metcalfe, J. C.** and **Quigley, M. B. C.** Keyhole stability in plasma arc welding. *Weld. J*., 1975, **11**, 401–404.

16 **Hu, B. X.** The study of controlling system of welding quality at all-position by using the arc sound in pulsed plasma arc welding of steel. *Welding*, 1980, **3**, 17–20.

17 **Agapakis, E.** and **Bolstad, J.** Vision sensing and processing system for monitoring and control of welding and other high luminosity processes. In Proceedings of International Robots and Vision Automation Conference, 1991, pp. 23–29.

18 **Martinez, L. F.** Front side keyhole detection in aluminum alloys. *Weld. J*., 1992, **5**, 49–52.

19 **Zheng, B., Wang, H. J.** and **Kovacevic, R.** Imaging the keyhole weld pool in variable polarity PAW of aluminum alloys. *Trans. ASME, J. Mfg Sci. Engng*, 1999 (accepted).

